Color Tuning of an Acidic Blue Dye by Intercalation into the Basic Interlayer Galleries of a Poly(allylamine)/Synthetic Fluoromica Nanocomposite

Hideo Hata,[†,‡,¶] Thomas E. Mallouk,[‡,*] and Kazuyuki Kuroda[¶,*]

Make-up & Hair Products Research and Development Center, Shiseido Co. Ltd., Hayabuchi 2-2-1, Tsuzuki-ku, Yokohama 224-8558, Japan, Department of Chemistry, The Pennsylvania State University, University Park, Pennsylvania 16802, and Department of Applied Chemistry, Faculty of Science and Engineering, Waseda University, Ohkubo 3-4-1, Shinjuku-ku, Tokyo 169-8555, Japan

Received October 1, 2008. Revised Manuscript Received January 20, 2009

The intercalation of an acidic blue dye, Brilliant Blue FCF, into poly(allylamine) (PAA)/synthetic fluoromica (Na-TSM) was investigated as a function of the reaction pH (1.5−12.0) and the loading of the polyelectrolyte and acidic dye. Surprisingly, the colored solids so obtained show a variety of colors from the original blue to yellow through green with only a slight increase in the reaction pH. At low and neutral pH (1.5−9.5), the acidic blue dye molecules were adsorbed/intercalated on/in PAA/Na-TSM mainly through electrostatic interactions between protonated amine groups on the PAA chains and sulfonate groups of the dye, resulting in the original blue color. UV−visible spectroscopic data hint that the adsorbed/intercalated dye molecules were aggregated. The color shifted to blue-green at pH 10.0 and finally to yellow at pH 12.0. At high pH, the PAA layers have lower charge density and the dye is well-dispersed within the interlayer galleries. The fraction of neutral primary amine groups increases with increasing reaction pH, and interaction of the neutral amine groups to the dye becomes the dominant driving force for intercalation. On the basis of these intercalation results at different pH and some control experiments, the pH-dependent color change of the intercalated dye appears to be caused by inhibition of the intramolecular interaction between N^+ in the dye conjugated system and a free sulfonate group.

Introduction

Many organic dyes are used in the food, cosmetics, medical, ink, and textile industries, as well as in electronics and optics, both for their color and for their other special optical properties. Acidic dyes often show more vivid and beautiful colors than traditional inorganic pigments such as iron oxides, iron blue, ultramarine blue, and trivalent chromium oxide and hydroxide. For food, medical, and cosmetics applications, however, only certain acidic dyes and their derivatives have been approved for use by the Food and Drug Administration (FDA) because of safety concerns.[1] Even for trivalent chromium compounds, which are the only green pigments globally permitted for cosmetics, the use is strictly restricted by the Pollutant Release and Transfer Register (PRTR). There are also practical limitations on using acidic dyes and their derivatives that arise from their low photostability and bleeding into solvents. Because several papers report improvements in the photostability of dyes adsorbed in/on inorganic host solids,[2,3] there is a practical motivation to investigate the properties of acidic dyes confined to the interlayer galleries of layered inorganic solids. In addition, the hue and extinction coefficients of dyes are generally controlled by the extent of their conjugated systems, as well as by chromophore, auxochrome, and intramolecular interactions. If it is possible to modulate these factors, one might expect that the color and absorption intensity of intercalated acidic dyes could be deliberately controlled, effectively giving rise to a new series of dyes and pigments. Despite the practical importance of these dyes, as far as we know, there have been no reports of deliberately using intercalation and adsorption as means of achieving color tuning.

High surface area inorganic solids have been widely investigated as host materials for organic molecules, and as building blocks for functional inorganic−organic nanostructures.[4−10] Among the available inorganic host materials, layered metal oxide nanosheets have been especially useful

* Corresponding author. E-mail: tom@chem.psu.edu (T.E.M.); kuroda@waseda.jp (K.K.).
† Shiseido Co. Ltd.
‡ The Pennsylvania State University.
¶ Waseda University.

(1) (a) Barel, A. O.; Paye, M.; Maibach, H. I. *Handbook of Cosmetic Science and Technology*; Marcel Dekker Inc.: New York, 2001. (b) Pakenham, L. C.; Murphy, E. G. *CTFA International Color Handbook*; The Cosmetic, Toiletry and Fragrance Association, Inc.: Washington D. C., 1985. (c) Marmion, D. M. *Handbook of U.S. Colorants for Foods, Drugs, and Cosmetics*, 2nd ed.; John Wiley & Sons; New York, 1984.
(2) Itoh, T.; Ishii, A.; Kodera, Y.; Matsushima, A.; Hiroto, M.; Nishimura, H.; Tsuzuki, T.; Kamachi, T.; Okura, I.; Inada, Y. *Bioconjugate Chem.* **1998**, *9*, 409.
(3) Itoh, T.; Yano, K.; Inada, Y.; Fukushima, Y. *J. Am. Chem. Soc.* **2002**, *124*, 13437.
(4) Sanchez, C.; Soler-Illia, G. J. A.; Robit, F.; Lalot, T.; Mayer, C. R.; Cabuil, V. *Chem. Mater.* **2001**, *13*, 3061.
(5) Ogawa, M.; Kuroda, K. *Chem. Rev.* **1995**, *95*, 399.
(6) Auerbach, S. M.; Carrado, K. A.; Duttam S. M. *Handbook of Layered Materials*; Marcel Dekker: New York, 2004.
(7) Kickelbick, G. *Hybrid Materials*; Wiley-VCH Verlag GmbH & Co. KGaA: Weinheim, Germany, 2007.

10.1021/cm802664j CCC: $40.75
Published on Web 02/19/2009

because of their high surface-to-volume ratio and chemical reactivity, especially intercalation and exfoliation reactions.[5−8] Mesoporous materials in the FSM,[11] KSW,[12] M41S,[13] HMS,[14] and SBA[15] families are also useful hosts for functional molecules. However, almost all of these layered and mesoporous solids have neutral or anionic frameworks, meaning that they are not good hosts for anionic guests. Layered double hydroxides (LDHs) are an exception because of their positive layer charge, but they have some important limitations as hosts for dyes. LDHs typically have a high charge density and the insertion of wedgelike organic anions has been needed to weaken the interlayer interaction for exfoliation,[16] although very recently it has been shown LDHs can be exfoliated in high dielectric organic solvents.[17] LDHs are also strongly basic and easily contaminated by atmospheric carbon dioxide, which leads to intercalated CO_3^{2-} ions. In addition, LDHs are thermally decomposed below 250 °C and are unstable under acidic conditions.[17f] Very recently, Sasaki and co-workers have reported a new class of rare earth hydroxides that are also lamellar anion exchangers.[18]

For these reasons, we recently developed a new general technique for inverting the layer charge of anionic host materials.[19,20] The process stems from the principle of layer-by-layer polyelectrolyte adsorption, which involves overcompensation of the layer charge.[21] With anionic layered hosts, charge inversion can be achieved by intercalating polycations with lower charge density than the enclosing sheets. The mismatch in charge density causes an excess of the polymer to intercalate, thereby introducing anion binding sites.[19a,20] The resulting polymer/nanosheet composites act as anion exchangers, as demonstrated by the intercalation of anionic dyes. When an acidic blue dye, Brilliant Blue FCF [disodium a-(4-N-ethyl-3-sulfonatobenzylamino phenyl)-a-(4-N-ethyl-3-sulfonatobenzylamino) cyclohaxa-2,5-dienylidene)-tolune-2-sulfonate] (Figure 1), was intercalated into fluoromica composites with a quarternary ammonium polyelectrolyte, the solid acquired the brilliant blue color of the dye, but minimal shifts in the absorption spectrum were observed.[19] Therefore, we anticipated that stronger host−guest interactions would be needed to modulate the absorption spectrum of the intercalated dye. In this context, we report here the effect of the protonation state of a preintercalated primary amine polymer on the absorption spectrum of the intercalated dye.

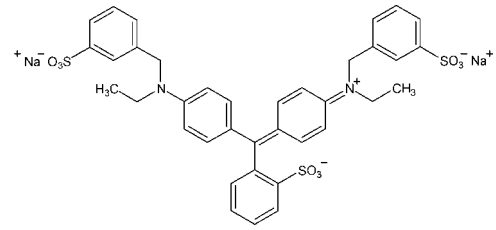

Figure 1. Chemical structure of Brilliant Blue FCF (B1).

We first studied the intercalation of B1 into poly(allylamine) (PAA)/fluoromica composites at pH 11.0, where PAA can adopt a thicker conformation because of the low polymer charge density, as a function of the PAA loading. We then investigated the effect of the reaction pH (1.5−12.0), which affects the protonation of the primary amine groups on PAA chains. Interestingly, the color of the intercalated solids changed from the original blue to light yellow through green with increasing reaction pH. At high pH (above 10.0), where the obtained dyed solids show the color change, the B1 aqueous solution shows no color change from the original blue color. So, it was suggested that the unique color change was induced by the intercalation into the polyamine/clay composites. We also report a series of experiments that suggest a possible mechanism for the color changes in the dye induced by changes in the state of protonation of the intercalated amine polymer.

Experimental Section

Materials. Sodium fluortetrasilicic mica (Na-TSM) with the chemical formula $Na_{0.66}Mg_{2.68}(Si_{3.98}Al_{0.02})O_{10.02}F_{1.96}$ and a cation exchange capacity (CEC) of 120 mequiv/100 g (ME-100, CO-OP Chemicals) was used as received. From the nitrogen adsorption, the Brunauer−Emmet−Teller (BET) surface area of Na-TSM is 3.3 m^2/g. The lateral size of the exfoliated Na-TSM nanosheets was around a few micrometers from the AFM images.[19a] Na-TSM is a synthetic 2:1 type layered silicate formed by the intercalation reaction of talc and Na_2SiF_6.[22] Poly(allylamine hydrochloride) (M_w

(8) Decher, G.; Schlenoff, J. B. *Multilayer Thin Films*; Wiley-VCH Verlag GmbH & Co. KGaA: Weinheim, Germany, 2003.
(9) Caruso, F. *Colloids and Colloid Assemblies*; Wiley-VCH Verlag GmbH & Co. KGaA: Weinheim, Germany, 2004.
(10) Rao, C. N. R.; Müller, A.; Cheetham, A. K. *Nanomaterials Chemistry*; Wiley-VCH Verlag GmbH & Co. KGaA: Weinheim, Germany, 2007.
(11) (a) Yanagisawa, T.; Shimizu, T.; Kuroda, K.; Kato, C. *Bull. Chem. Soc. Jpn.* **1990**, *63*, 988. (b) Inagaki, S.; Fukushima, Y.; Kuroda, K. *J. Chem. Soc., Chem. Commun.* **1993**, 680.
(12) Kimura, T.; Kamata, T.; Fujiwara, M.; Takano, Y.; Kaneda, M.; Sakamoto, Y.; Terasaki, O.; Sugahara, Y.; Kuroda, K. *Angew. Chem., Int. Ed.* **2000**, *39*, 3855.
(13) (a) Kresge, C. T.; Leonowicz, M. E.; Roth, W. J.; Vartuli, J. C.; Beck, J. S. *Nature* **1992**, *359*, 710. (b) Beck, J. S.; Vartuli, J. C.; Roth, W. J.; Leonowicz, M. E.; Kresge, C. T.; Schmitt, K. D.; Chu, C. T.-W.; Olson, D. H.; Sheppard, E. W.; McCullen, S. B.; Higgins, J. B.; Schlenker, J. L. *J. Am. Chem. Soc.* **1992**, *114*, 10834.
(14) Tanev, P. T.; Pinnavaia, T. J. *Science* **1995**, *267*, 865.
(15) (a) Huo, Q.; Margolese, D. I.; Stucky, G. D. *Chem. Mater.* **1996**, *8*, 1147. (b) Zhao, D.; Feng, J.; Huo, Q.; Melosh, N.; Fredrickson, G. H.; Chmelka, B. F.; Stucky, G. D. *Science* **1998**, *279*, 548.
(16) (a) Adachi-Pagano, M.; Forano, C.; Besse, J.-P. *Chem. Commun.* **2000**, 91. (b) Leroux, F.; Adachi-Pagano, M.; Intissar, M.; Chauvie're, S.; Forano, C.; Besse, J.-P. *J. Mater. Chem.* **2001**, *11*, 105. (c) Hibino, T.; Jones, W. *J. Mater. Chem.* **2001**, *11*, 1321. (d) Hibino, T. *Chem. Mater.* **2004**, *16*, 5482. (e) Hibino, T.; Kobayashi, M. *J. Mater. Chem.* **2005**, *15*, 653.
(17) (a) Li, L.; Ma, R.; Ebina, Y.; Iyi, N.; Sasaki, T. *Chem. Mater.* **2005**, *17*, 4386. (b) Liu, Z.; Ma, R.; Osada, M.; Iyi, N.; Ebina, Y.; Takada, K.; Sasaki, T. *J. Am. Chem. Soc.* **2006**, *128*, 4872. (c) Liu, Z.; Ma, R.; Ebina, Y.; Iyi, N.; Takada, K.; Sasaki, T. *Langmuir* **2007**, *23*, 861. (d) Ma, R.; Liu, Z.; Li, L.; Iyi, N.; Sasaki, T. *J. Mater. Chem.* **2006**, *16*, 3809. (e) Li, L.; Ma, R.; Ebina, Y.; Fukuda, K.; Takada, K.; Sasaki, T. *J. Am. Chem. Soc.* **2007**, *129*, 8000. (f) Kobayashi, Y.; Ke, X.; Hata, H.; Schiffer, P.; Mallouk, T. E. *Chem. Mater.* **2008**, *20*, 2374.
(18) Geng, F.; Matsushita, Y.; Ma, R.; Xin, H.; Tanaka, M.; Izumi, F.; Iyi, N.; Sasaki, T. *J. Am. Chem. Soc.* **2008**, *130*, 16344.
(19) (a) Hata, H.; Kobayashi, Y.; Mallouk, T. E. *Chem. Mater.* **2007**, *19*, 79. (b) Hata, H.; Kobayashi, Y.; Mallouk, T. E. *MRS Symp. Proc.* **2007**, *988E*, 0988-QQ03−03.
(20) (a) Hata, H.; Kubo, S.; Kobayashi, Y.; Mallouk, T. E. *J. Am. Chem. Soc.* **2007**, *129*, 3064. (b) Hata, H.; Kobayashi, Y.; Salama, M.; Malek, R.; Mallouk, T. E. *Chem. Mater.* **2007**, *19*, 6588.
(21) (a) Decher, G.; Hong, J.-D.; Schmitt, J. *Thin Solid Films* **1992**, *210/211*, 504. Decher, G. *Science* **1997**, *277*, 1232.
(22) (a) Tateyama, H.; Nishimura, S.; Tsunematsu, K.; Jinnai, K.; Adachi, Y.; Kimura, M. *Clays Clay Miner.* **1992**, *40*, 180. (b) Tateyama, H.; Tsunematsu, K.; Noma, H.; Adachi, Y.; Takeuchi, H.; Kohyama, N. *J. Am. Ceram. Soc.* **1996**, *79*, 3321.

= 15 000, abbreviated PAA) and poly(diallyldimethylammonium chloride) (M_w < 100 000, abbreviated PDDA) were purchased from Sigma-Aldrich. Brilliant Blue FCF (FD & C Blue No. 1, abbreviated B1) was purchased from Kishi Kasei Co., Ltd. (Yokohama, Japan). Light Green SF (denoted as G205) was purchased from Wako Pure Chemical Industries, Ltd. (Osaka, Japan). FD & C Yellow No. 5 (Tartrazin, denoted as Y5, 80% purity) was obtained from Sigma-Aldrich. Water was deionized to a resistivity of 18 MΩ-cm using a Nanopure water purification system. All other compounds were used as received from commercial sources.

Intercalation of PAA into Na-TSM. PAA is a weak base polyelectrolyte, so the degree of the protonation of the primary amine groups depends on the reaction pH, which dominates the conformation of the polyelectrolyte on anionic substrates.[8,23] In our previous report,[20b] we found that PAA intercalated into Na-TSM at pH 12.0 adopts a thicker conformation that allows intercalation of guest species. Therefore, we first studied the intercalation of the dye B1 into nanocomposites formed by PAA intercalation at pH 12.0.

Na-TSM (0.75 g) was added to 74.25 g of water, and the dispersion was stirred overnight at room temperature to ensure adequate exfoliation of Na-TSM. PAA aqueous solutions (25 g) of appropriate concentration were added to the Na-TSM dispersions, and pH was adjusted to 12.0−12.1 using a 10 M aqueous NaOH, followed by vigorous agitation for 1 day at 25 °C. The amount of PAA added to the dispersion was 0.9 (1/1), 2.7 (3/1), or 4.5 (5/1) mmol. The numbers in parentheses indicate the initial ratio of amine groups in the PAA to the cation exchange capacity (CEC) of Na-TSM. After the reaction, the solid product was separated by centrifugation and washed twice with 75 g of dilute NaOH at pH 12.0−12.1 to remove excess polymer. Finally, the samples were dried at 60 °C for 1−2 days and ground to powders. These nanocomposites are designated PAA/Na-TSM (*n*), where *n* denotes the initial ratio of amine groups in the PAA to the cation exchange capacity (CEC) of Na-TSM.

We found in our previous study that intercalated PAA gradually adopts a monolayer conformation as the pH is decreased, likely driven by electrostatic attraction between protonated amine groups and the enclosing anionic sheets. In the process, some PAA is eliminated from the interlayer galleries.[20b] To accurately calculate the dye content in B1/PAA/Na-TSMs made at different pH values, one must know the PAA content at the relevant pH. Therefore, PAA/Na-TSM (5/1) made at pH 12.0−12.1 was washed three times in aqueous dispersions whose pH levels had been adjusted with NaOH or HCl to 1.5−1.6, 3.0−3.1, 7.0−7.1, 8.0−8.1, 9.0−9.1, 9.5−9.6, 10.0−10.1, 10.5−10.6, 11.0−11.1, 11.5−11.6, or 12.0−12.1.

Intercalation of the Acidic Dye into Polyelectrolyte/Na-TSM Nanocomposites at Different Loadings of PAA. Na-TSM (0.75 g) was added to 74.25 g of water, and the dispersion was stirred for 1 day at room temperature. Twenty-five grams of an aqueous solution containing 0.9, 2.7, or 4.5 mmol of PAA was then added. The pH was adjusted to 12.0−12.1 using 10 M NaOH, followed by vigorous stirring for 1 day at 25 °C. The dispersions were then centrifuged, and the products were washed twice with 100 g of dilute NaOH at pH 12.0−12.1. Water was added to the wet nanocomposite to a total weight of 75.0 g, and 25.0 g of an aqueous solution containing 0.9 mmol of B1 was added at pH 11.0−11.1. The selection of this pH was based on our previous optimization of the intercalation of gold nanoparticles into PAA/Na-TSM.[20b] The dispersion was vigorously stirred for one day at room temperature, followed by centrifugation and washing three times with water at pH 11.0−11.1 to remove excess B1. Finally the sample was dried at 60 °C for 1 or 2 days and ground to a powder. The products obtained were designated B1/PAA/Na-TSM (*n*), where *n* again indicates the initial molar ratio of the dye and the amine groups in the polymer to the CEC of Na-TSM.

Intercalation of Acidic Dye into Polyelectrolyte/Na-TSM Nanocomposites as a Function of pH. Wet PAA/Na-TSM (5/1), prepared at pH 12.0−12.1 as described above, was redispersed in water to a total weight of 75 g. A total of 25 g of 36 mM aqueous B1 solution was then added to each dispersion; the pH was again adjusted to pH 12.0−12.1, 11.5−11.6, 11.0−11.1, 10.5−10.6, 10.0−10.1, 9.5−9.6, 9.0−9.1, 8.0−8.1, 7.0−7.1, 3.0−3.1, and 1.5−1.6 with aqueous NaOH or HCl. The mixtures were vigorously stirred for 1 day at room temperature. After the reaction, the dispersions were centrifuged, and the solid products were washed three times with water at the previously set pH values. Finally, the dye-loaded samples were dried at 60 °C for 1−2 days and ground to powders. Of course, one might expect the some side effects of conducting the reaction at extremely high or low pH on the crystallinity of Na-TSM nanosheets. From the XRD patterns (from $2\theta = 10-60$ deg) of the original Na-TSM and B1/PAA/Na-TSMs obtained at pH 1.5−1.6, 3.0−3.1, 7.0−7.1, 10.0−10.1, and 12.0−12.1 (see the Supporting Information, Figure S10), there is no apparent difference in the profile of each sample; in addition, the diffraction peak due to the (020) reflection,[24] which indicates the crystallinity of the nanosheet itself, was clearly observed at $d = 0.45$ nm in each XRD pattern. Therefore, although the edge of the clay nanosheets might be eroded at pH 1.5 or 12.0, the structure of the clay nanosheet was basically maintained after the reaction. For the intercalation of the G205 and Y5 dyes into PAA/Na-TSM (5/1), the same experimental procedure was used at pH 3.0−3.1 or 11.0−11.1. Hereafter, we will simplify the designation of the reaction pH range; for example, pH 7.0−7.1 is described as pH 7.0.

Instrumentation. X-ray powder diffraction (XRD) patterns were obtained with a Mac Science M03X-HF22 diffractometer (Mn filtered Fe Kα ($\lambda = 0.1936$ nm) radiation) and a JEOL JDX-3500 X-ray diffractometer system (monochromated Cu $K\alpha_1$ ($\lambda = 0.1541$ nm) radiation). Infrared spectra were obtained by the KBr method using a Thermo Electron Corporation Nicolet 6700 FT-IR spectrometer. UV−vis absorption spectra were obtained on a Hitachi U-3500 spectrophotometer. Because we could not completely redisperse PAA/Na-TSM or B1/PAA/Na-TSM after drying, wet gel samples which were washed but not dried were used to obtain UV−vis absorption spectra. CHN analysis was performed with a Perkin-Elmar 2400 CHNS/O analyzer. The amount of B1 adsorbed in B1/PAA/Na-TSM under each set of reaction conditions was estimated from the difference in analytical carbon contents of B1/PAA/Na-TSM and PAA/Na-TSM prepared under the same conditions of pH and PAA concentration. Zeta-potential measurements were conducted with a Brookhaven Instruments Zeta PALS at 25 °C. The pH dependence of the zeta-potential was obtained by adjusting the pH with 0.01 M aqueous NaOH or HCl. Nitrogen Brunauer−Emmet−Teller (BET) surface area measurements were performed by using a Micromeritics ASAP 2010 instrument. The hue in the Munsell color system and diffuse reflectance spectra of the product powders were measured with a quartz-windowed vessel for powders in a Konica-Minolta CM 2600d spectrophotometer. Prior to measuring the color dimensions, the measurement system was normalized with an attached standard white reflecting plate as a reference.

(23) (a) Shiratori, S. S.; Rubner, M. F. *Macromolecules* **2000**, *33*, 4213. (b) Choi, J.; Rubner, M. F. *Macromolecules* **2005**, *38*, 116.

(24) Inoue, K.; Tateyama, H.; Noma, H.; Nishimura, S. *Clay Sci.* **2001**, *11*, 391.

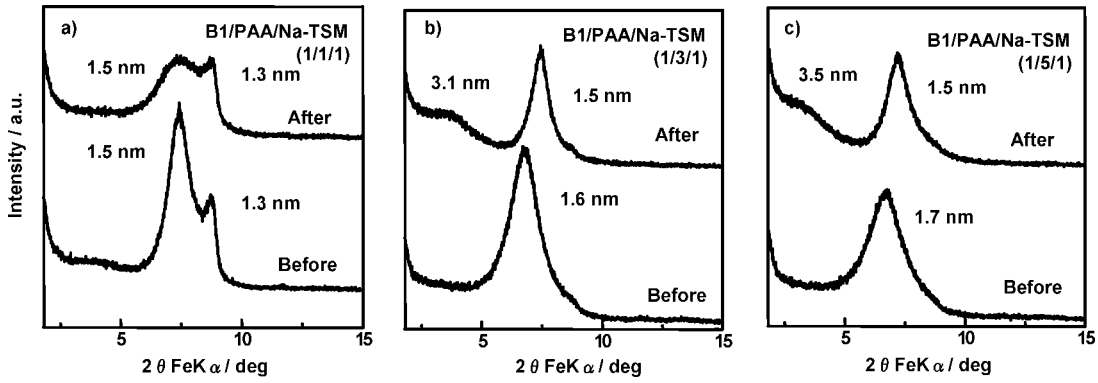

Figure 2. XRD patterns of B1/PAA/Na-TSMs before and after the intercalation of B1 at pH 11.0; B1/PAA/Na-TSM = (a) 1/1/1, (b) 1/3/1, and (c) 1/5/1.

Table 1. Analytical Data for PAA/Na-TSM and B1/PAA/Na-TSM Nanocomposites Synthesized at pH 11.0

B1/PAA/Na-TSM initial molar ratio	amount of PAA adsorbed (mmol/100 g of clay)	amount of B1 adsorbed (mmol/100 g of clay)	PAA/Na-TSM molar ratio	B1/PAA molar ratio
1/1/1	110	2.40	0.92	0.022
1/3/1	352	10.4	2.93	0.030
1/5/1	377	11.4	3.14	0.030

Results and Discussion

1. Intercalation of B1 Molecules into PAA/Na-TSMs at Different PAA Loadings under Basic and Acidic Conditions. In the XRD pattern of PAA/Na-TSM (1/1) (Figure 2a), the peak due to the basal spacing is observed at 1.5 nm alongside the peak due to the hydrated Na-TSM starting material at 1.3 nm. Subtracting the thickness of the silicate layer of Na-TSM (1.0 nm),[25] the gallery height of PAA/Na-TSM (1/1) is estimated to be 0.5 nm, which corresponds to a monolayer of intercalated polymer chains.[23] As the initial concentration of PAA is increased, the *d*-spacing of the PAA/Na-TSMs increases to 1.7 nm (panels b and c in Figure 2). Considering that the thickness of stretched PAA chains estimated to be around 0.5 nm, the expansion of the interlayer distance is so short that a bilayer structure cannot be adopted by the intercalated PAA; therefore, the accommodated PAA chains may coil but only in the plane of the interlayer gallery. The observed loading corresponds to intercalation of amine groups slightly in excess of the CEC of the enclosing sheets, and the excess amount increases as the PAA/Na-TSM ratio and gallery height increase.[20] CHN analytical data (Table 1) show that the amount of PAA is 110 mmol/100 g of clay in PAA/Na-TSM (1/1), which increases to 377 mmol/100 g of clay at n = 5/1. The latter value is almost three times the CEC of Na-TSM. In our previous report, we studied PDDA adsorption onto a nonexfoliative potassium fluoromica (K-FM)[26] to quantify the effect of the external surface on polyelectrolyte adsorption; in that case, the amount of adsorbed polycation was estimated to be only 2.3 mmol/100g clay. This allows us to conclude that almost all of the PAA is intercalated into the Na-TSM interlayer galleries. The FT-IR spectra of PAA/Na-TSM (1/1 and 5/1) are shown in Figure S1. At n = 1/1, a shoulder due to the antisymmetric stretching vibration of neutral amine groups was observed at 3373 cm^{-1}. Considering that PAA/Na-TSM made at pH 12.0 contains no Cl^- regardless of PAA loading,[20b] most amine groups in PAA/Na-TSM (1/1) are ionized and interact with the anionic clay surface to compensate the anionic layer charge. On the other hand, when n was increased to 5/1, prominent bands due to neutral amine groups were observed at 3377 (υ_{as}) cm^{-1}. This is consistent with a higher density of neutral amine groups at higher loading. Although the observed *d*-spacing of PAA/Na-TSMs are slightly larger than those in our previous report, the basic trends are the same in terms of structure and degree of protonation.[20b]

After the intercalation reactions of B1 at pH 11.0, surprisingly, all of the solid products (n = 1/1/1, 1/3/1, and 1/5/1) showed a significant color change from the original blue to light green. (see Figure S2 in the Supporting Information) In the XRD pattern of B1/PAA/Na-TSM (1/1/1) (Figure 2a), the peak attributed to the basal spacing becomes broader after intercalation of B1, but there was no discernible peak shift. In contrast, in the patterns of the (1/3/1) and (1/5/1) samples, new peaks were observed at *d*-spacings of 3.1 and 3.5 nm, corresponding to increases in the gallery height of 1.5 and 1.8 nm, respectively. In addition, the diffraction patterns show a new phase with smaller layer spacing (1.5 nm) than that of the original PAA/Na-TSM. In our previous study of Na-TSM intercalated with PDDA, the same peak splitting was observed after the B1 intercalation.[19] As noted before, this phase separation is likely driven not by elimination of polyelectrolyte molecules from Na-TSM but by the higher lattice energy of the more compact phase, which contains no B1 molecules.[19] The analytical B1 contents of B1/PAA/Na-TSM (1/1/1, 1/3/1, and 1/5/1) were 2.40, 10.4, and 11.4 mmol/100 g of clay, respectively (Table 1). The B1/PAA molar ratios were 0.022 (1/1/1), 0.030 (1/3/1), and

(25) In the XRD pattern of the original Na-TSM, two different peaks were observed at *d*-spacing of 1.2 and 1.0 nm, and these two peaks were attributed to hydrated and dehydrated layers, respectively. Hence, the basal spacing of the silicate layer was taken to be 1.0 nm.

(26) Synthetic unexpandable potassium fluoromica, $KMg_3AlSi_3O_{10}F_2$ (K-FM), was purchased from Topy Ind. Co. The BET surface area of K-FM was 5.5 m^2/g from the nitrogen adsorption measurement.

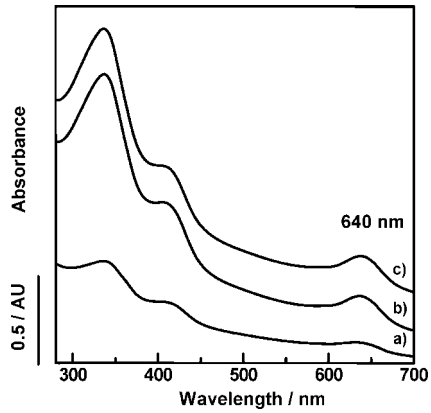

Figure 3. UV−vis absorption spectra of 0.02 wt % aqueous dispersions of B1/PAA/Na-TSM = (a) 1/1/1, (b) 1/3/1, and (c) 1/5/1.

0.030 (1/5/1), which are only about one tenth of the ratio of B1/PAA/Na-TSM (1/5/1) made at pH 3.0, where most of amine groups are fully protonated. From zeta potential measurements of PAA/Na-TSM (5/1) as a function of pH (see the Supporting Information, Figure S3), the isoelectric point of the PAA/Na-TSM is about pH 11.0. This indicates that most of the amine groups in the interlayer galleries are neutral above pH 11.0, and hence PAA/Na-TSM made at high pH is not expected to have high anion exchange capacity.[20]

Figure 3 shows the UV−visible absorption spectra of 0.02 wt % aqueous dispersions of B1/PAA/Na-TSM (1/1/1, 1/3/1, and 1/5/1) obtained at pH 11.0. In each spectrum, the original absorption peak at 629 nm shifted to 640 nm. In the case of B1/PDDA/Na-TSM, intercalated B1 molecules showed a similar red-shift in the peak at 629−650 nm, reflecting the hydrophobic environment of the interlayer galleries of PAA/Na-TSMs. However, in B1/PAA/Na-TSM, the intensity of the peak at 640 nm is substantially lower than in the original spectrum of B1 in aqueous solution (see the Supporting Information, Figure S6), and the absorbance in blue region is significantly increased. This spectral change corresponds to the color change from blue to green. Considering the structural differences between the quaternary ammonium polyelectrolyte (PDDA) and the basic polyelectrolyte (PAA), it is likely that the neutral amine groups on the intercalated PAA dominate this color change. The mechanism of the color change will be discussed in the following section.

2. Effect of pH on the Intercalation of B1 into PAA/Na-TSM. To investigate the relationship between the protonation state of intercalated PAA and the electronic spectra of the intercalation compounds, we varied the pH of solutions from which B1 was intercalated into PAA/Na-TSM (5/1) nanocomposites that had been prepared at pH 12.0. Surprisingly, depending on the reaction pH, the resulting B1/PAA/Na-TSM powders showed a wide range of colors (Figure 4). The intercalation compounds were purple-blue (PB) when they were prepared at pH 1.5, blue (B) between pH 3.0 and 8.0, blue-green to light green at pH 9.0−10.5, and faint yellow above pH 11. Almost the same color change was also observed in the corresponding B1/PAA/Na-TSM dispersions before being dried into the powders (see the Supporting Information, Figure S11). Figure 5 shows XRD patterns of B1/PAA/Na-TSM (1/5/1) obtained at pH 1.5−12.0. In the XRD patterns of the solids intercalated at low pH, weak and broad diffraction peaks were observed at approximately 1.5−1.7 nm in addition to some ambiguous broad shoulders in the lower angle side, indicating a turbostratic restacking of the sheets during the intercalation of B1. For nanocomposites intercalated at pH 10.0 and above, the basal spacing is approximately constant at 1.5 nm, but an additional low angle peak begins to appear at $d = 3.5$ nm. This peak (also evident in panels b and c in Figure 2) was attributed above to an intercalation compound that contains both neutral PAA chains and B1 molecules. Table 2 shows that the amount of PAA retained is lowest at pH 1.5−3.0, where the polymer is highly charged and intercalates as a monolayer between the negatively charged silicate sheets. At higher pH, the PAA loading gradually increases and above pH 10, the amount of intercalated PAA is approximately twice that at low pH, consistent with the larger gallery height observed. At the same time, the amount of anionic B1 that is intercalated into PAA/Na-TSM falls from 77−78 mmol/100 g at pH 1.5−3.1 to about 10 mmol/100 g above pH 10.5. In our previous report, we determined the adsorption of B1 onto a PDDA/K-FM composite, where only the external surface could be used as the adsorption site. The amount of B1 adsorbed on PDDA/K-FM was only 0.57 mmol/100 g,[19a] indicating that the interlayer galleries are the predominant site for intercalation of B1 into PAA/Na-TSM, even under high pH conditions. The trend in B1 loading corresponds to the pH dependence of the zeta-potential of PAA/Na-TSM (see the Supporting Information, Figure S3), supporting the idea that the amount of positive charge on the PAA/Na-TSM surface controls the loading of B1 molecules below pH 10. Interestingly, at pH 10.5 and above, where the zeta potential of the composite is nearly neutral or negative, there is a relatively constant loading of B1 molecules. The intercalation of negatively charged B1 into the anionic host implies that some other kind of interaction drives the intercalation of B1 molecules at high pH.

Infrared and UV−visible spectra of the nanocomposites are informative in understanding the state of protonation of the intercalated polymer and the nature of the interaction between PAA and B1. In the FT-IR spectra of PAA/Na-TSMs (5/1) washed at pH 1.5−11.0 (see the Supporting Information, Figure S4), bands attributed to neutral primary amine groups at 1568 (υ_s) and 3377 (υ_{as}) cm^{-1} gradually diminish with decreasing pH. At pH 7.0, no apparent band due to the neutral primary amines can be observed, indicating that PAA amine groups are mostly protonated when the reaction pH is below 7.0. The FT-IR spectra of crystalline B1 and B1/PAA/Na-TSM (1/5/1) obtained at pH 1.5−12.0 are compared in Figure 6. In the B1 crystal, the two antisymmetric stretching bands of the $S(=O)_2$ groups of B1 are observed at 1168 and 1190 cm^{-1}; these can be attributed to sulfonate groups associated with Na^+ and free sulfonate, respectively (see the B1 structure shown in Figure 1). In the spectra of B1/PAA/Na-TSM (1/5/1) intercalated at pH 1.5−9.5, the spectra in the fingerprint region are quite similar to that of the B1 crystal. The antisymmetric stretching bands

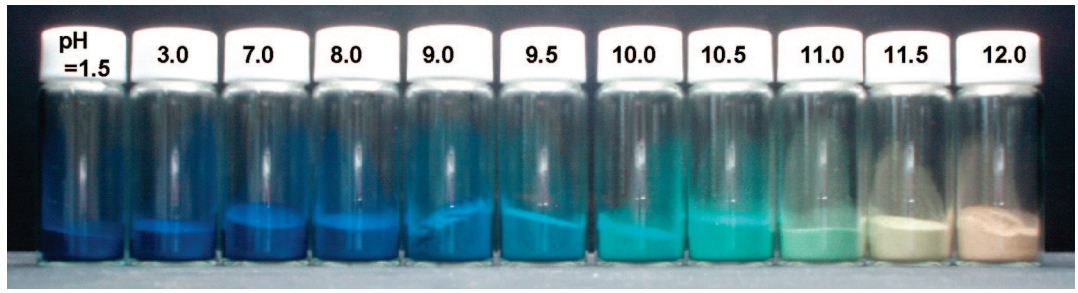

Figure 4. Photograph of B1/PAA/Na-TSMs (1/5/1) obtained at pH 1.5−12.0.

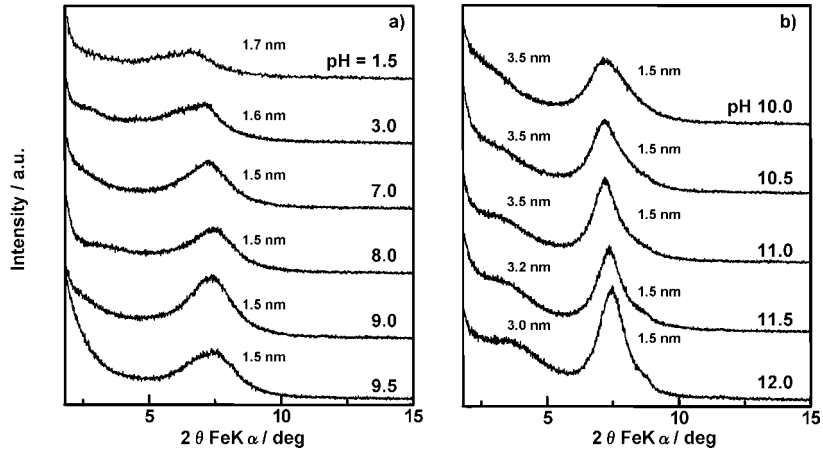

Figure 5. XRD patterns of B1/PAA/Na-TSM (1/5/1) obtained at pH of (a) 1.5−9.5 and (b) 10.0 − 12.0.

Table 2. Analytical Data for PAA/Na-TSM (5/1) Washed at pH 1.5−12.0 and dye/PAA/Na-TSM Intercalated under Different pH Conditions

	pH	amount of PAA adsorbed (mmol/100 g of clay)	amount of B1 adsorbed (mmol/100 g of clay)	PAA/Na-TSM molar ratio	B1/PAA molar ratio	hue	hue after dehydration
B1/PAA/Na-TSM (1/5/1)	1.5−1.6	198	77.0	1.65	0.389	6.26 PB	
	3.0−3.1	194	78.4	1.61	0.405	5.18 PB	7.28 PB
	7.0−7.1	242	68.5	2.01	0.283	4.83 PB	5.72 PB
	8.0−8.1	309	57.3	2.58	0.185	3.34 PB	
	9.0−9.1	348	37.9	2.90	0.109	6.99 B	
	9.5−9.6	351	25.4	2.93	0.072	1.80 B	
	10.0−10.1	371	14.9	3.09	0.040	5.46 BG	3.52 BG
	10.5−10.6	380	10.5	3.17	0.027	0.97 BG	
	11.0−11.1	377	10.2	3.14	0.027	1.26 G	
	11.5−11.6	379	10.2	3.16	0.027	0.41 Y	
	12.0−12.1	378	8.19	3.15	0.022	1.05 Y	3.81 Y
G 205/PAA/Na-TSM (1/5/1)	3.0−3.1	194	89.7	1.61	0.463	1.21 BG	
	11.0−11.1	377	9.59	3.14	0.025	0.68 Y	
Y5/PAA/Na-TSM (1/5/1)	3.0−3.1	194	77.2	1.61	0.399	8.45 YR	
	11.0−11.1	377	1.88	3.14	0.005	3.82 Y	

of the sulfonate groups appear at 1172−1174 and 1190 cm^{-1}, respectively. This implies the presence of some free sulfonate groups and some that are associated with protonated amine groups.

Figure 7 shows UV−visible absorption spectra of 0.02 wt% aqueous dispersions and diffuse reflectance spectra of B1/PAA/Na-TSM (1/5/1) intercalated at pH 1.5−12.0. In the absorption spectra of the aqueous dispersions (Figure 7A), the blue B1/PAA/Na-TSM (1/5/1) nanocomposites obtained at pH 1.5 to 9.5 show a broad absorption band with shoulder peaks at 583, 630, and 678 nm. There are many reports on absorption shifts due to dye aggregation. Cyanine dyes can make both *H* and *J*, aggregates, giving bands that are respectively blue- and red-shifted compared with the monomer spectra.[27] Therefore, immobilized B1 molecules appear to form such aggregates in B1/PAA/Na-TSMs. On the other hand, in the diffuse reflectance spectra of the corresponding B1/PAA/Na-TSM (1/5/1) powders, the absorption maxima were observed at 560 nm below pH 8.0, and gradually shifted to 630 nm as the reaction pH was increased to 9.5. Comparing the spectra of the dispersions and powders below pH 9.5, it appears that the *H* type aggregation form is more predominant in the dried powders, or that cointercalated water inhibits dye aggregation. Under more basic conditions, the color of obtained powders changes from blue (B) to blue-green (BG), green (G), finally shifted yellow (Y) (Table 2 and Figure 4). In the FT-IR spectra of B1/PAA/Na-TSM (1/5/1) obtained at pH 10.0−12.0 (Figure 6), the antisymmetric stretching bands of $S(=O)_2$ that were originally at 1168 and

(27) Mishra, A.; Behera, R. K.; Behera, P. K.; Mishra, B. K.; Behera, G. B. *Chem. Rev.* **2000**, *100*, 1973.

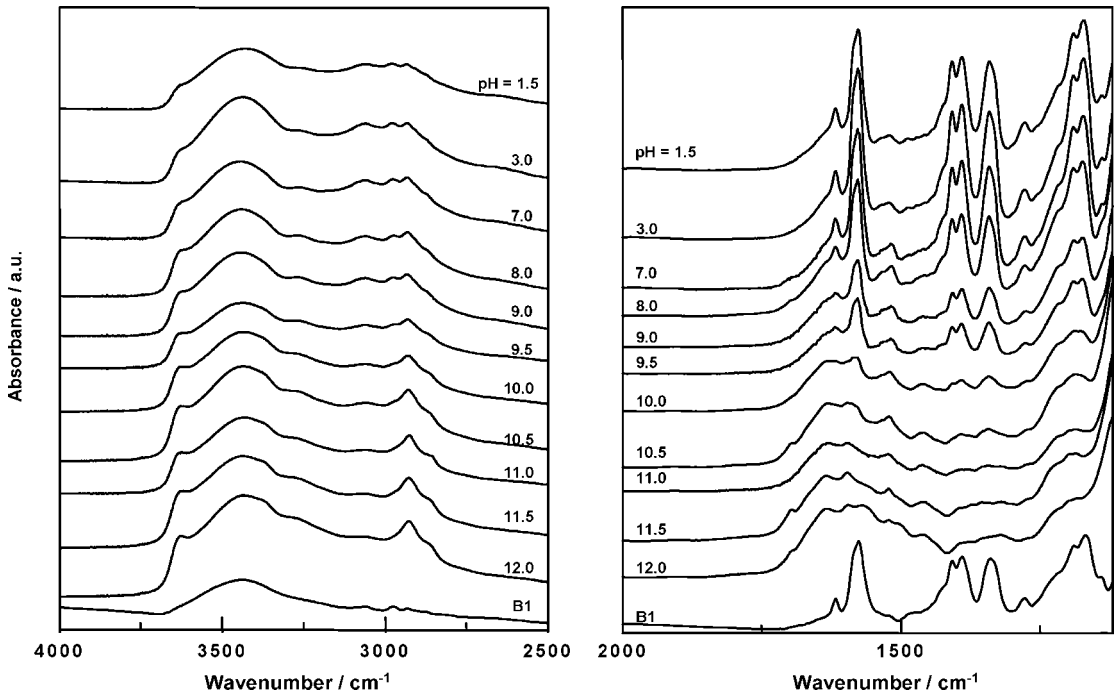

Figure 6. FT-IR spectra of B1 and B1/PAA/Na-TSM (1/5/1) obtained at pH 1.5−12.0.

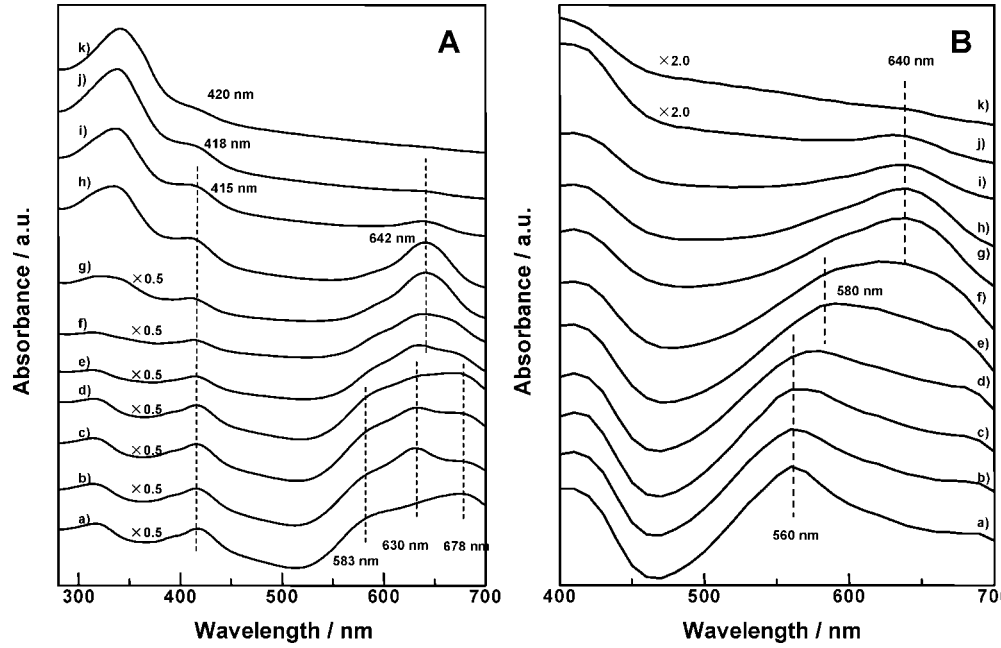

Figure 7. UV−vis absorption spectra of (A) 0.02 wt % aqueous dispersions and (B) diffused reflectance spectra of B1/PAA/Na-TSM (1/5/1) at pH (a) 1.5, (b) 3.0, (c) 7.0, (d) 8.0, (e) 9.0, (f) 9.5, (g) 10.0, (h) 10.5, (i) 11.0, (j) 11.5, and (k) 12.0.

1190 cm^{-1} merge into one broadband around 1184−1191 cm^{-1}, indicating that all the sulfonate groups of B1 are in the same kind of environment. At pH 10.0, the UV−visible absorption maximum is 642 nm, and the shoulders at 583 and 678 nm that were observed pH 1.5−9.5 are not present. At higher pH, the absorption peak at 642 nm decreases and finally disappears at pH 12.0; at the same time, the peaks in the blue to UV region increase and show a small red-shift. The same tendency of the absorption in the red region was observed in the corresponding diffuse reflectance spectra of dyed powders. These observations are consistent with the dispersion of B1 molecules in the intercalated polymer without significant interactions with protonated amine groups. At high pH, the electrostatic interactions between PAA and B1 are negligible, and the interactions between the neutral amine groups of PAA and B1 appear to control both the intercalation and the color change.

It is well-known that the color of dyes in heterogeneous media is strongly dependent on the water content. In addition, we have already reported that B1 molecules are site-selectively accommodated into the hydrated layers of PDDA/Na-TSM composites, and the interlayer water can be removed by heating at 120 °C for 1 day.[19a] Therefore, the effect of coadsorbed water content within the interlayer space of B1/PAA/Na-TSMs on the color was also investigated by dehydration. From the XRD patterns of B1/PAA/Na-TSMs

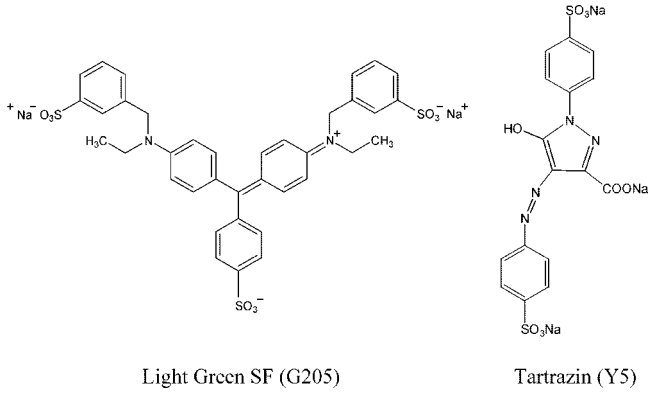

Figure 8. Structures of Light Green SF (G205) and Tartrazin (Y5).

(1/5/1) at pH 1.5 and 12.0 heated at 120 °C for 1 day, a decrease in interlayer spacing was observed, indicating the removal of water from the interlayer. As for the color of dyed solids after heating, very little change of the hue is observed (Table 2). In the diffuse reflectance spectra of B1/PAA/Na-TSM (1/5/1) prepared at pH 1.5 and 10.0 (see the Supporting Information, Figure S12a and b), the absorption maxima (λ_{max}) in the red region shift slightly to the lower wavelength side, and the absorption peaks become broad, especially in B1/PAA/Na-TSM (1/5/1) at pH 10.0, implying the aggregation of B1 molecules. At pH 12.0 (see the Supporting Information, Figure S12c), no apparent peak shift was observed, although the absorption intensity in the blue region increased, which corresponds to the hue of the powder becoming more yellowish after heating. From these results, one can conclude that coadsorbed water affects the absorption behavior of the dye molecules, but it cannot cause the huge color change from blue to yellow through green observed in this study.

3. Mechanism of the Color Change of the Blue Dye in PAA/Na-TSM. In the previous section, we showed that the interaction between the neutral primary amine groups of PAA and the dye molecules causes an unexpected color change. Here, we discuss the mechanism of this color change by comparing with B1 in aqueous solutions, and with the results of intercalation reactions of structurally related dyes.

Aqueous solutions of B1 show color changes from blue to yellow through green as the pH is decreased from 10.7 to 0.0 by adding HCl (see the Supporting Information, Figure S5). UV−visible spectra of these solutions (0.025 mM) are shown in the Supporting Information, Figure S6. Between pH 12.0 and 3.0, the dye retains its original blue color. Below pH 2.0, the intensity of the peak in red region (629 nm) gradually decreases. At pH 0.25, the band centered at 629 nm becomes weak, and a broad absorption peak at 424 nm is observed, corresponding to a green solution. In a concentrated HCl solution, B1 is yellow, and only a broad absorption peak at 438 nm is observed. These color changes can be reversed by increasing the pH. In the B1 molecule (Figure 1), there is an intramolecular electrostatic interaction between N^+ in the aromatic π-system and the deprotonated SO_3^- groups. Protonation of the sulfonate (SO_3H) group at pH 0.25−0.0 results in the color change from blue to yellow through green. In the closely related green acidic dye, Light Green SF (G205) (Figure 8), the central SO_3^- group is located at the para position of one of the phenyl rings, and this is the only structural difference between G205 and B1, which has the SO_3^- group in the ortho position. In the UV−visible spectra of aqueous B1 and G205 solutions, absorption maxima are observed at 629 nm, but the intensity is lower for G205 than it is for B1. In the G205 structure, there is a greater distance between the N^+ and the central SO_3^- group, resulting in a weaker intramolecular electrostatic interaction. Hence, we hypothesize that the intramolecular electrostatic interaction enhances the absorption intensity in red region of B1, resulting in its strong blue color across a wide range of pH values.

When G205 was intercalated into PAA/Na-TSM (5/1) at pH 3.0, the resulting intercalation compound G205/PAA/Na-TSM (1/5/1) retained the deep green color of the dye (see the Supporting Information, Figure S9). XRD patterns and UV−visible spectra (see the Supporting Information, Figures S7 and S8) indicate that the intercalation behavior of G205 is very similar to that of B1.[28] At pH 3.0, the absorption peak of intercalated G205 at 629 nm was broadened because of aggregation of the dye molecules. On the other hand, at pH 11.0, the G205 was intercalated into the basic interlayer galleries and the color changed from green to yellow (see the Supporting Information, Figure S9). The amount of G205 intercalated and the molar ratio of dye to PAA at pH 3.0 and 11.0 followed the same trends B1/PAA/Na-TSMs (Table 2). This implies that acidic dyes having intramolecular electrostatic interactions in the π-system show significant color changes when they are intercalated into PAA/Na-TSM under basic conditions where PAA is deprotonated.

We also examined the intercalation of a yellow acidic dye (Y5), which has no intramolecular interaction between charged groups, into PAA/Na-TSM (5/1) at pH 3.0 and 11.0. In contrast to the B1 and G205 systems, Y5/PAA/Na-TSMs were yellow at both high and low pH (see Table 2 and the Supporting Information, Figure S9). In the XRD patterns of the products, a broad shoulder peak attributed to the Y5 intercalated phase was observed at pH 3.0. The amounts of intercalated Y5 in Y5/PAA/Na-TSM at pH 3.0 (77.2 mmol/100 g clay) and the molar ratio of Y5 to PAA (0.399) were very close to those of B1 and G205 in the analogous intercalation compounds. In contrast, at pH of 11.0, there was no evident low angle XRD peak corresponding to a Y5/PAA/Na-TSM intercalated phase. The Y5 content and Y5/PAA molar ratio at pH 11.0 were 1.88 mmol/100 g clay and 0.005, which are much lower than of the values obtained with B1 and G205 systems. This indicates that Y5, which has higher anionic charge density than B1 or G205 under

(28) In the XRD pattern of G205/PAA/Na-TSM (1/5/1) obtained at pH 3.0, some ambiguous broad shoulder diffraction peaks were observed, indicating the turbostatic restacking of the solids during the G205 intercalation. In the UV−vis absorption spectrum of the solids at pH 3.0, a broad absorption band was observed in the red region. This suggests the aggregation of G205 molecules on/in the host (PAA/Na-TSM (5/1)). On the other hand, in the system of the intercalation of G205 into PAA/Na-TSM (5/1) at pH 12.0, a prominent broad diffraction peak was observed in the lower angle side of the original PAA/Na-TSM (5/1) in the XRD patterns. In the UV-vis absorption spectrum, the absorption intensity of the peak in the red region was substantially decreased, and the peak in blue to UV region increased, which corresponds to the hue change.

basic conditions, is not well-accommodated by the largely neutral PAA polymer in the interlayer galleries.

On the basis of these results, we can hypothesize that the unexpected color change of B1 in B1/PAA/Na-TSMs under basic conditions arises from interactions between neutral PAA and the π-system of the dye. The role of the polymer may be to screen the intramolecular electrostatic interaction, possibly by interaction of the PAA nonbonding electron pairs with the π-conjugated system of the dye. In aqueous solutions under strongly acidic conditions, B1 is protonated and this also disrupts the intramolecular electrostatic interaction between N^+ and SO_3^-, resulting in a similar color change. In the intercalation compounds under acidic conditions, most of the amine groups on the intercalated PAA chains are protonated and can interact electrostatically with the SO_3^- groups of B1, in a manner similar to the interaction of Na^+ in the B1 crystal. Under these conditions, B1 retains its blue color.

Conclusions

With the view of creating new color pigments, we investigated the intercalation of an acidic blue dye, B1, into PAA/Na-TSM nanocomposites as a function of the loadings of both polyelectrolyte and dye and the reaction pH. An unexpected color change was observed under basic conditions, where the intercalated PAA is predominantly neutral. In contrast, the intercalation compounds made at lower pH, where some of the amine groups of PAA are protonated, are deep blue and the color resembles that of B1 in neutral or basic aqueous solutions. Similar trends are followed for the acidic G205 dye and the anomalous color changes can be interpreted in terms of the interaction between neutral PAA and the intercalated dye molecules, possibly through screening of intramolecular electrostatic interactions.

Because there has been a need for a new green pigment with high chroma saturation and no restrictions on its use, this green B1/PAA/Na-TSM compounds are a possible replacement for conventional trivalent chromium pigments whose hue is around 1.0−2.0 blue green. It is also possible that cointercalation with neutral amine polymers might be effective for color tuning of other acidic dyes with intramolecular electrostatic interactions, such as Sulpho Rhodamine B (Acid Red); if so, this method could lead to an interesting new family of pigments. In addition, anionic dye molecules are of interest for applications in artificial photosynthesis, photodynamic therapy, and biomedical imaging. However, there are few reports so far of the intercalation of anionic dyes into negatively charged inorganic nanosheets.[29] The availability of basic nanocomposite hosts thus potentially opens a new class of materials for these applications.

Acknowledgment. This work was supported in part by a Grant-in-Aid for Scientific Research (18350110), by the Global COE program "Practical Chemical Wisdom" from MEXT, Japan, and by the National Science Foundation (CHE-0616450).

Supporting Information Available: FT-IR spectra of PAA/Na-TSMs, photographs of B1/PAA/Na-TSMs, G205/PAA/Na-TSMs, Y5/PAA/Na-TSMs, B1 solutions at different pHs, and aqueous suspensions of B1/PAA/Na-TSMs, pH dependence of the zeta potential of PAA/Na-TSM, UV visible absorption spectra of B1 solutions at different pHs and suspensions of G205/PAA/Na-TSMs and Y5/PAA/Na-TSMs, XRD patterns of G205/PAA/Na-TSMs, Y5/PAA/Na-TSMs, Na-TSM, and B1/PAA/Na-TSMs, and diffused reflectance spectra of B1/PAA/Na-TSMs before and after heating (PDF). This material is available free of charge via the Internet at http://pubs.acs.org.

CM802664J

(29) (a) Yui, T.; Uppili, S. R.; Shimada, T.; Tryk, D. A.; Yoshida, H.; Inoue, H. *Langmuir* **2002**, *18*, 4232. (b) Lucia, L. A.; Yui, T.; Sasai, R.; Takagi, S.; Takagi, K.; Yoshida, H.; Whitten, D. G.; Inoue, H. *J. Phys. Chem. B* **2003**, *107*, 3789.